Supporting Information for

Metastable Intermediates in Amorphous Titanium Oxide: A Hidden Role Leading to Ultra-Stable Photoanode Protection

Yanhao Yu,[†] [‡] Congli Sun,[†] Xin Yin, Jun Li, Shiyao Cao, Chenyu Zhang, Paul M. Voyles*, Xudong Wang*

Department of Materials Science and Engineering, University of Wisconsin-Madison, Madison, WI 53706, USA.

[†] These authors contributed equally to this work.

[‡] Present address: John A. Paulson School of Engineering and Applied Sciences, Harvard University, Cambridge, MA, 02138, USA.

∗ Email: xudong.wang@wisc.edu (XW); paul.voyles@wisc.edu (PMV)

Methods

TiO_2 and Ni thin film deposition

Atomic layer deposition of TiO_2 on Si substrate: The 380 μm-thick, 3 inch-diameter, single-side polished, <100> oriented, phosphorus doped, n-type Si wafers with resistivity of 1-10 Ω·cm were used for all TiO_2 film deposition and photoelectrochemcial (PEC) devices. Wafers were cleaned sequentially in the ultrasonic bath of acetone, isopropanol and deionized (DI) water for 20 min. Prior to TiO_2 depositions, Si wafers were immersed in 5 wt% HF to remove the native oxide. TiO_2 coating was conducted in a homemade atomic layer deposition (ALD) system following reported procedures.[1] The target substrate was loaded on a quartz tube and placed at the position 5 cm away from the precursor inlet nozzle. N_2 gas with a flow rate of 40 sccm was introduced into the chamber to serve as the carrier gas. The system's base pressure was kept at 3.8 Torr. The chamber temperature was maintained at 160 °C for most experiments. For results shown in Figure S12b, d, e, the deposition temperature was adjusted to 120 °C. $TiCl_4$ (Sigma-Aldrich, 99.9%) and DI H_2O vapors were pulsed into the deposition chamber separately with a pulsing time of 0.5 s and separated by 60 s N_2 purging. Therefore, one deposition cycles involves 0.5 s of H_2O pulse + 60 s of N_2 purging + 0.5 s of $TiCl_4$ pulse + 60 s of N_2 purging with a $TiCl_4$ pressure change of 120 millitorr (chamber pressure difference before and after ALD valve open). The chamber was cooled down naturally under N_2 flow after growth. 24 nm and 2.5 nm-thick TiO_2 coatings were received after 400 and 40 ALD cycles, respectively, corresponding to a growth rate of 0.06 nm per cycles. $TiCl_4$ was chosen as the precursor, rather than rather than organometallic Ti precursors, since $TiCl_4$ can avoid the involvement of big organic molecules, which may dim the structure and property comparison between intermediates and amorphous/crystalline counterparts. Free of organic byproducts could improve the accuracy of

our observation and analysis of the metastable intermediates. Moreover, halide precursor may promote the nucleation of ALD TiO_2 and thereafter enrich the pool of intermediates. This will help us quickly locate the target and distinguish the performance dependency.

Sputtering of Ni on TiO_2 coated Si: The 12 nm Ni films were deposited on TiO_2 coated Si through sputtering using a CVC 601 DC sputtering system. During the deposition the substrate was rotated with a speed of 5 rpm. The flow rate of argon gas was 25 sccm. The deposition time, pressure, power, voltage, current were 120 s, 10 militorr, 200 W, ~300 V, ~0.65 A, respectively.

PEC Electrode fabrication

The back sides of Si wafer were first scratched with a diamond scribe (to remove the native oxides), and then were coated with Ga/In eutectic mixture and connected to a metal lead, forming an Ohmic back contact. Silver paint was then used to affix the lead. After drying in the fume hood, the entire back side and partial front side of the Si electrodes were encapsulated in Epoxy (Loctite, 9460), establishing an exposed active area of ~0.1 cm^2. Calibrated digital images and ImageJ were used to determine the geometrical area of the exposed electrode surface defined by epoxy.

Electrochemical measurements

The PEC tests were carried out in a typical three-electrode electrochemical setup with $Si/TiO_2/Ni$ as the working electrode, a Pt wire as the counter electrode and a Hg/HgO electrode as the reference electrode. The electrolyte was 1 M NaOH aqueous solution. During the cyclic voltammetry (CV) and chronoamperometry scanning, working electrodes were illuminated by a 150 W Xenon lamp coupled with an AM 1.5 global filter with a light intensity of 100 $mW \cdot cm^{-2}$ (one sun). Chronoamperometry curves were measured at a constant external bias of 1.8 V vs.

RHE. Hg/HgO was converted to RHE using the following relationship: E(RHE) = E(Hg/HgO) + 0.098 V + 0.059 × pH. All electrochemical curves were recorded using an Autolab PGSTAT302N station.

Material characterizations

SEM characterizations: Scanning electron microscopy (SEM) images were acquired on a Zeiss LEO 1530 field-emission microscope with a gun voltage of 5 kV and a working distance of ~3 mm. SEM energy dispersive X-ray spectroscopy (EDS) was performed at a voltage of 10 kV and a working distance of ~8 mm. The cross-sectional SEM images were obtained by physically breaking the PEC device and then choosing the piece of wafer with sharp fresh edge. To improve picture quality, the front side of the sample was electrically connected to the SEM stage through a conductive carbon tape.

AFM measurements: Atomic Force Microscopy (AFM) characterizations were conducted using a XE-70 Park System. The current-AFM (c-AFM) procedure was similar to previously reported c-AFM process.[3] For the c-AFM, the 24 and 2.5 nm-thick TiO_2 films were grown on 380 μm-thick, boron heavily doped, single-side polished, <100> oriented, p type wafer with a resistivity of 0.001-0.005 Ω·cm. The Si wafer were then electrically glued onto a steel disc using Ga/In eutectic and silver paste, creating an Ohmic contact between Si and steel disc, similar to the PEC electrode fabrication case. The AFM was operated in the contact mode with a platinum cantilevers and a complete circuit was formed by AFM tip-TiO_2/Si-AFM stage. The current mappings were recorded under a constant bias of -3 V while the tomography images were probed simultaneously. The individual current-voltage curves were collected by swiping the bias between 3 V to -3 V.

STEM sample preparation: Cross sectional scanning transmission electron microscopy (STEM) samples were prepared by in-situ lift out using a Zeiss Auriga focused ion beam (FIB). The final FIB milling voltage was reduced to 2 kV to minimize damage from implanted Ga. The final milling was performed on a Fischione 1050 Nano mill equipment with accelerating voltage of 0.5 kV and an incident angle of 10˚.

STEM and EELS observations: STEM and electron energy loss microscopy (EELS) experiments were performed on a FEI Titan microscope with a CEOS probe aberration-corrector operated at 200 keV. The probe semi-angle was 24.5 mrad and the probe current was ~25 pA. The estimated probe size was less than 1 Å. Annular bright field (ABF) STEM image were collected by Gatan 805 BF/DF detector spanning 5.7 to 12.6 mrad. EEL spectrum image were recorded with GIF 865 spectrometer, with energy dispersion of 0.2 eV/pixel, which allowed the simultaneous visualization of the Ti-L and O-K EELS edges. The energy resolution was 0.85 eV measured from the full width at half maximum of zero-loss peak. Quantifications were calculated using the Digital Micrograph implementation of the standard quantification method.

Supporting Figures

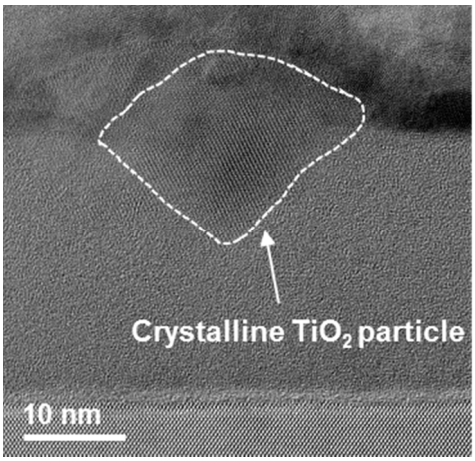

Figure S1. A cross-sectional ABF STEM image of a crystalline particle in the ADL grown amorphous TiO_2 thin film on Si substrate. The white dashed line marks the crystalline particle boundary.

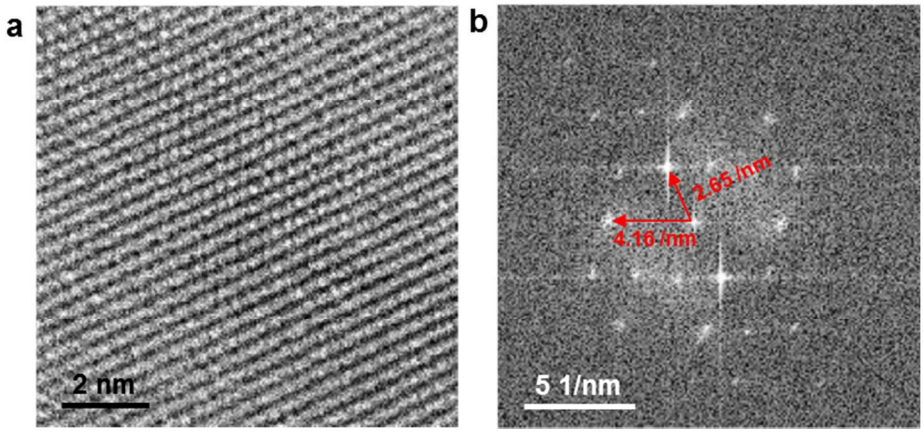

Figure S2. (**a**) The high-resolution ABF STEM image inside the crystalline particle in Figure 1J. (**b**) Fast Fourier transform (FFT) of (a), identifying two lattice distances of 0.24 and 0.38 nm, which match well with the (004) and (011) planes of anatase TiO_2, respectively.

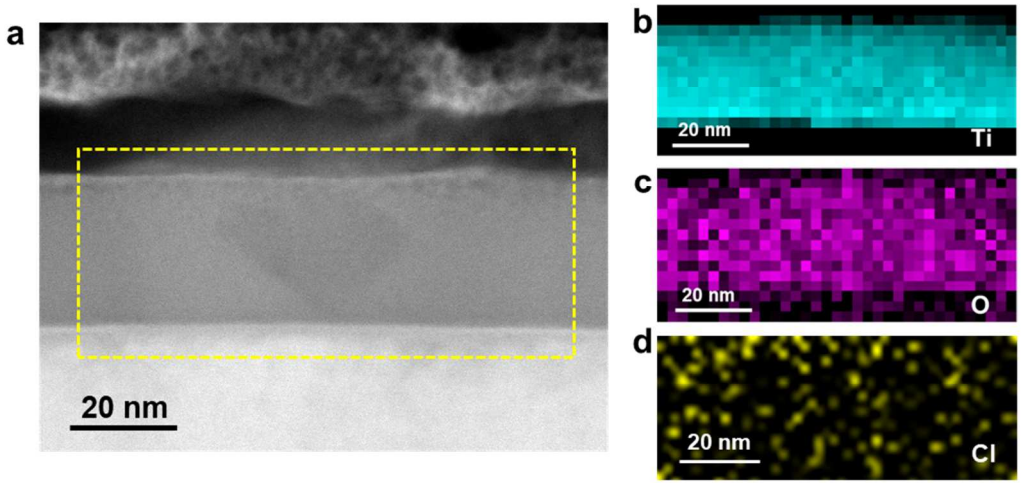

Figure S3. (**a**) The cross-sectional ABF STEM image of the TiO_2 thin film, featuring a dark region in the center of TiO_2 film (the same picture shown in Figure 1c). (**b-d**) STEM EELS mappings of Ti (b), O (c) and Cl (d) elements, illustrating uniform Ti and O distributions within the detecting region. Cl concentration was less than 2% according to the EELS quantification.

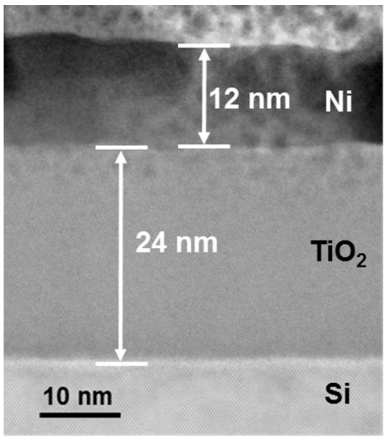

Figure S4. A cross-sectional ABF STEM image of the Si/TiO_2/Ni electrode.

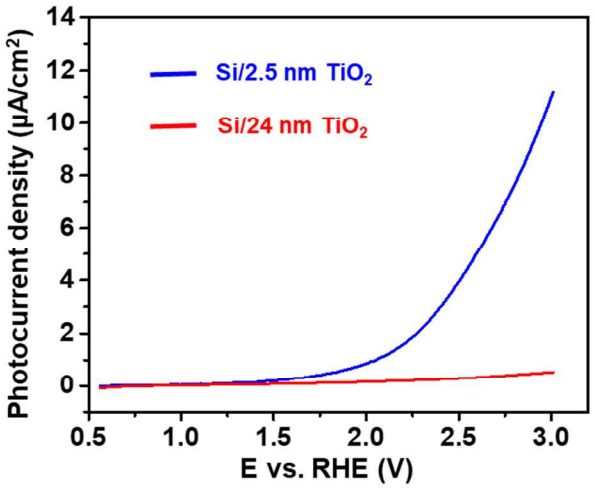

Figure S5. The photocurrent density-voltage curves of Si/2.5 nm and Si/24 nm TiO_2 electrodes under 1 sun illumination. The small photocurrent density validates the necessary of introducing the catalyst layer.

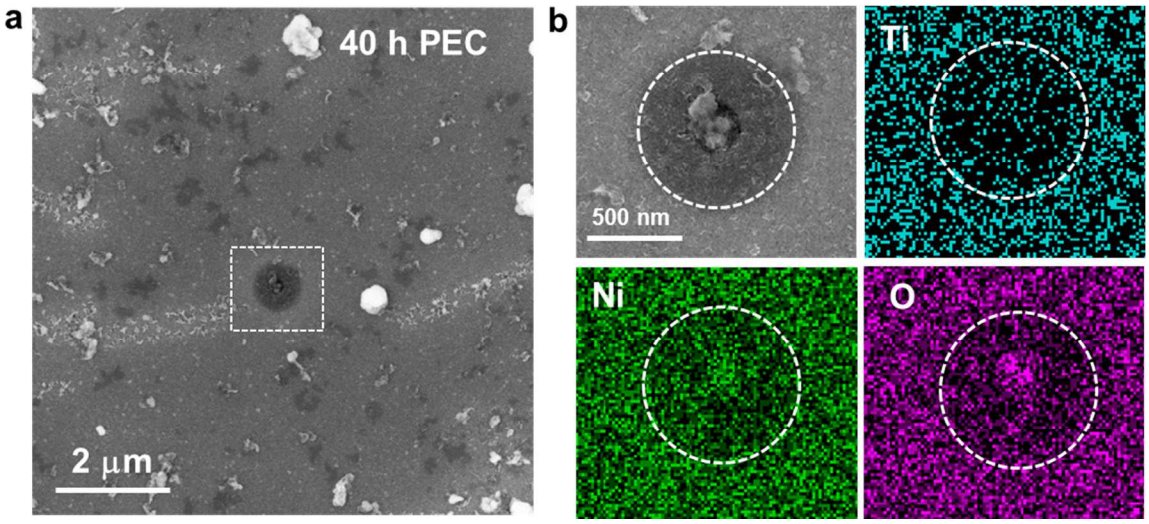

Figure S6. (**a**) A top-view SEM image of the Si/TiO_2/Ni electrode after 40 hours PEC reaction. (**b**) An amplified SEM image and corresponding elemental mapping through SEM EDS for the circular damage (white dashed square) observed in (a). The Ti signal inside the circle (white dashed area) suggests the existence of TiO_2 in the corrosion region.

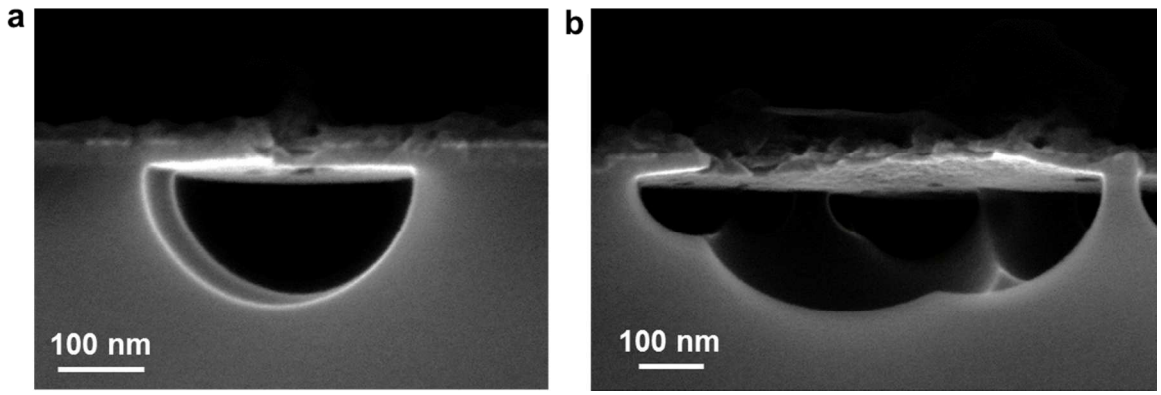

Figure S7. Cross-sectional SEM images of the Si/TiO_2/Ni electrode after 80 hours PEC reactions at the locations with a single (**a**) and an interconnected (**b**) Si etching area.

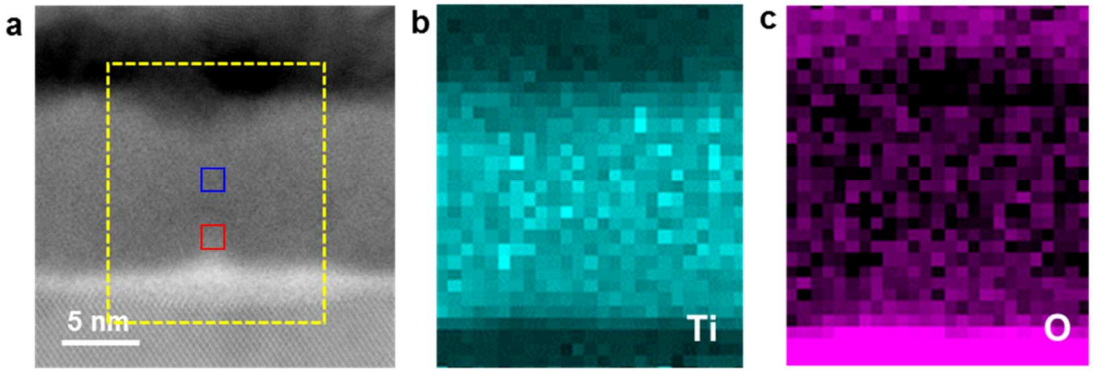

Figure S8. (**a**) A cross-sectional ABF STEM image of the initial etching location in the Si/TiO_2/Ni electrode after 40 hours PEC reaction (the same picture shown in Figure 1K). (**b**, **c**) STEM EELS mapping of Ti (b) and O (c) elements, showing a deficiency of Ti at the top and bottom areas, and a concentrated O at the bottom area. The relative Ti:O ratios at the middle (blue square) and bottom (red square) portions were quantified to be 32.12:67.88 and 28.83:71.17, confirming the O enrichment at the bottom region.

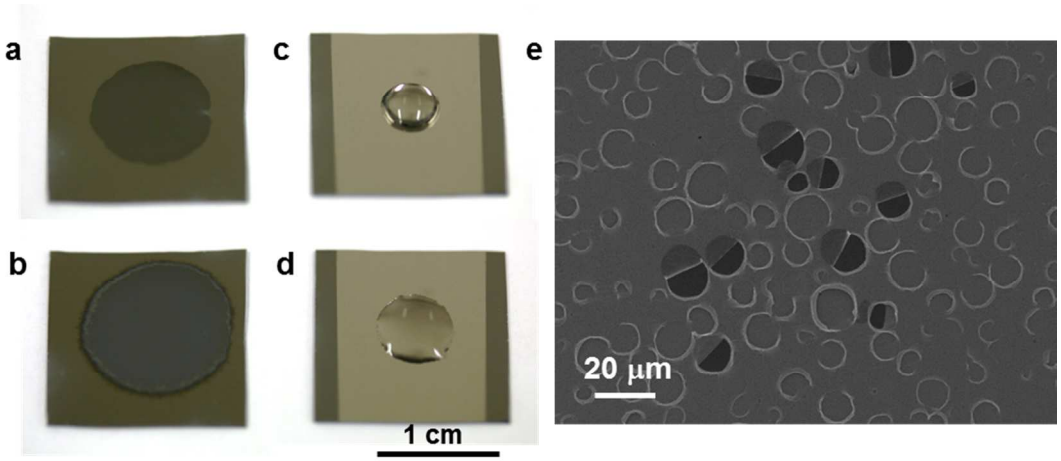

Figure S9. Etching of amorphous TiO_2 in 10 M NaOH aqueous solution. (**a**) A digital image of a 10 M NaOH droplet on the top of 24 nm-thick amorphous TiO_2 thin film on a Si wafer. The circular dark contrast featured the droplet area. (**b**) A digital image of the droplet-covered area in (a) after 2 hours. The droplet expanded to a larger circle before drying out in the air. Within the droplet-covered area, the substrate color was changed from light brown (representing uniform TiO_2 coating on Si) to light grey (the color of bare Si surface), indicating the thorough dissolution of TiO_2. (**c**) The digital image of a 10 M NaOH droplet on the top of Ni metal coated 24 nm-thick amorphous TiO_2 thin film on a Si wafer. The different droplet diameter in (a) and (c) was caused by the different hydrophilicity of TiO_2 and Ni surfaces. (**d**) The digital image of the droplet in (c) after 2 hours. (**e**) The top-view SEM image of the droplet area shown in (d). A number of circular-shape damages were formed, similar to the corrosion of $Si/TiO_2/Ni$ electrode after PEC reaction shown in Figure 1e.

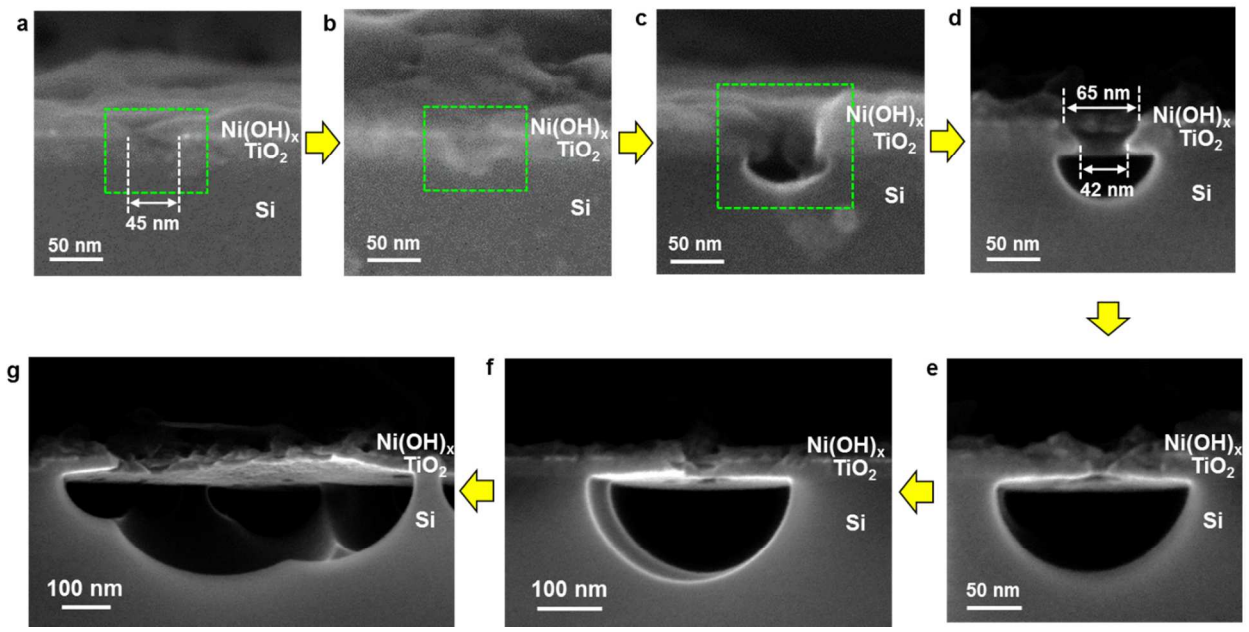

Figure S10. A series of cross-sectional SEM images, showing seven individual moments covering the electrode damaging process. (**a**) The initial etching of TiO_2 at the intermediate area. An embryo orifice with a lateral size of ~45 nm can be observed. (**b**) The TiO_2 orifice was etched through and a slight damage to Si was resulted. The TiO_2 orifice acted as a transport channel for hydroxyl group, resulting in the etching of Si. (**c**) The TiO_2 orifice was further evolved and a cavity-like damage was formed in Si. (**d**) The TiO_2 orifice was remained at the same size, suggesting the etching of TiO_2 was ceased after the development of the orifice. The Si cavity was further expanded due to the continuous hydroxyl etching. (**e**,**f**) The size of Si cavity was additionally increased, producing a suspended TiO_2 thin film on the top of the cavity. The size of the orifice was remained at the same scale, reinforcing that TiO_2 etching was terminated after fully consuming the intermediate area. (**g**) Several Si cavities were interconnected, forming a micro-size damage area. At this location, the top TiO_2 film was partially destroyed, presumably caused by surface tension or large local strain. The green dashed square marked the etching locations at the initial stages.

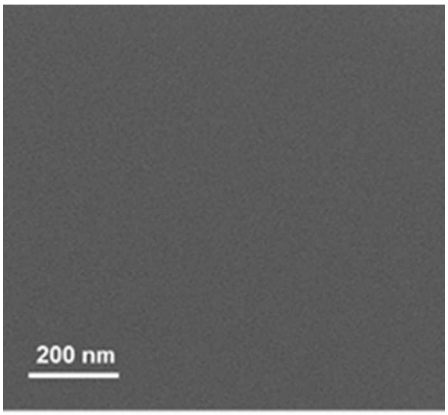

Figure S11. A top-view SEM image of the 2.5 nm TiO_2 thin film on a Si substrate.

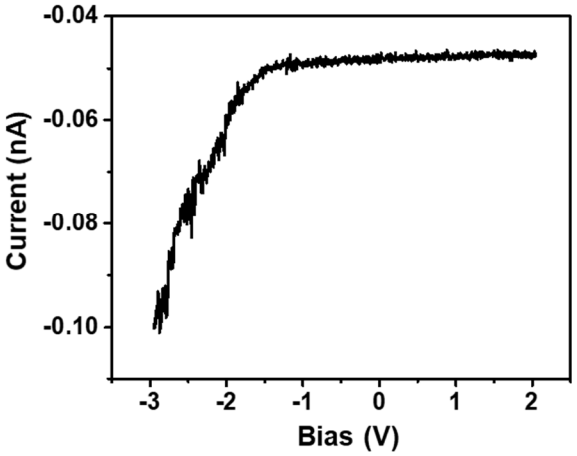

Figure S12. The local I-V characteristic of the 2.5 nm TiO_2.

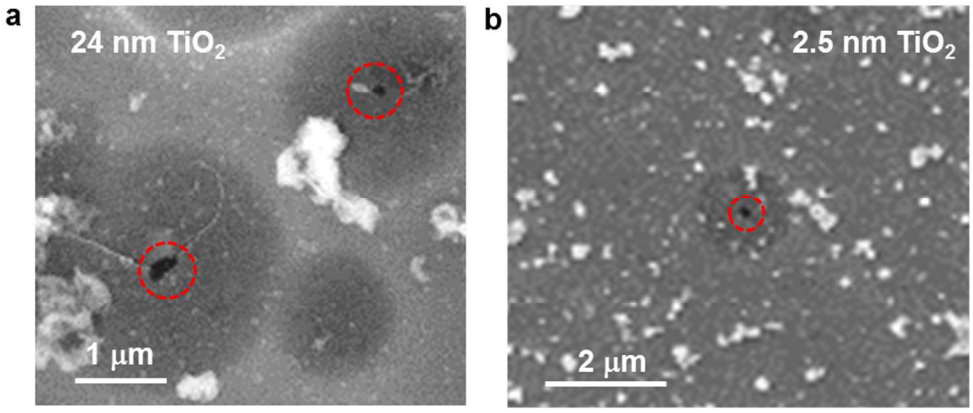

Figure S13. (**a**) Top view SEM image of the 24 nm TiO_2-protected electrodes after 80 hours PEC reaction. (**b**) Top view SEM image of the 2.5 nm TiO_2-protected electrodes after 110 hours PEC reaction. The picture (a) and (b) are the amplified version of insets in Figure3c and 4f, respectively.

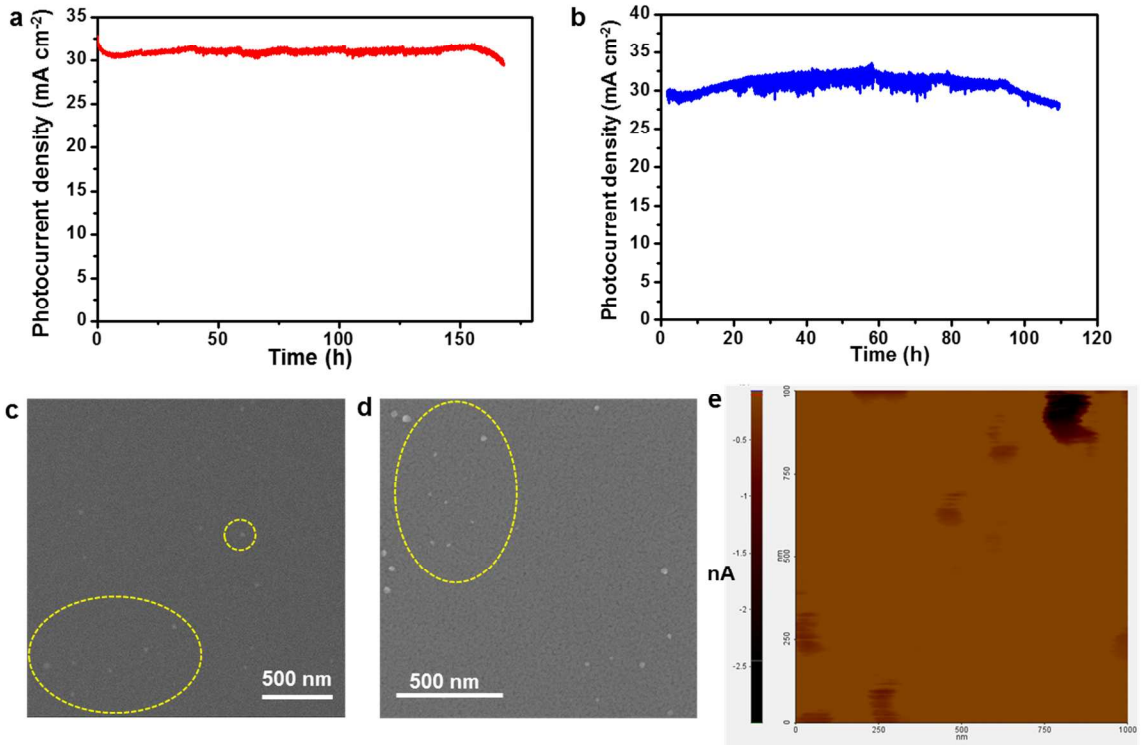

Figure S14. (**a, b**) Chronoamperometry of the Si/TiO_2/Ni electrodes with a 10 nm TiO_2 thin film deposited at 160 °C (a) and a 24 nm TiO_2 thin film deposited at 120 °C (b) measured in 1.0 M

NaOH aqueous solution under one sun illumination. (**c, d**) Top-view SEM image of the 160 °C, 10 nm (c) and 120 °C, 24 nm (d) TiO_2 thin films. Yellow circles highlight the areas with crystalline particles. (**e**) C-AFM of 120 °C, 24 nm TiO_2 thin film, showing the less amount of intermediates compared to the 160 °C, 24 nm TiO_2 thin film.

Supporting Tables

Table S1. Average current of amorphous areas, particles and intermediates detected by conductive AFM.

	Amorphous areas	Particles	Intermediates
Average current of 10 units (nA)	0.1	0.2	2.8

Table S2. Reproducibility of 2.5 nm TiO_2 protected Si electrodes

Samples	Plateau current ($mA \cdot cm^{-2}$)	Onset potential (V)	Hours before degradation (hour)
Sample 1	30.6	1.30	560
Sample 2	29.8	1.32	517
Sample 3	31.2	1.32	460

Reference

41. Yu, Y.; Yin, X.; Kvit, A.; Wang, X. *Nano Lett.* **2014,** 14, 2528-2535.
42. Liu, B.; Aydil, E. S. *J. Am. Chem. Soc.* **2009,** 131, 3985-3990.

43. Warren, S. C.; Voitchovsky, K.; Dotan, H.; Leroy, C. M.; Cornuz, M.; Stellacci, F.; Hebert, C.; Rothschild, A.; Gratzel, M. *Nat. Mater.* **2013,** 12, 842-849.